Solution of two-temperature thermal diffusion model of laser–metal interactions

Vatsya, S.R.; Virk, Kuljit S.

Publisher's version / Version de l'éditeur:
https://doi.org/10.2351/1.1619998
Journal of Laser Applications, 15, 4, pp. 273-278, 2003-10-21

Solution of two-temperature thermal diffusion model of laser-metal interactions

S.R. Vatsya and Kuljit S. Virk

Integrated Manufacturing Technologies Institute
National Research Council of Canada
800 Collip Circle, London, Ontario, Canada, N6G 4X8

Abstract

The two temperature coupled equations, modelling thermal diffusion during laser-induced ablation of metals, are solved under the assumptions that the electron and the lattice heat capacities, and the thermal conductivity remain constant in the process. In view of its practical value, the solution is initially obtained for the energy sources with a Gaussian distribution. The solution is then generalized to include a larger class of source terms for comparison with other results. Present analysis is valid under less restrictive conditions than frequently imposed in the literature. In particular, the solution is valid for realistic source terms and describes the process for ultra-short to nanosecond pulse-width regimes. More general results obtained here retain the attractive features of other approximate solutions available elsewhere and reduce to them under the respective conditions. Predictions of the present model agree well with the experimental observations reported in the literature.

1.0 Introduction

High power lasers with short pulse widths are widely used for micro-machining because of their ability to machine surfaces with high accuracy and precision with little damage to the underlying material. Metals and their alloys are commonly processed with lasers. Models under varying assumptions have been proposed to describe the response of metals to laser irradiation[1-6]. In brief, the laser-energy absorbed by the thermal electrons is transferred to the lattice subsystem by collisions between the energized electrons and the atoms[1]. This transfer of the energy is modeled in terms of the electron-phonon coupling term, which is directly proportional to the temperature difference between the electrons and the lattice subsystems[2]. The ablation depth is obtained by integrating the velocity of the evaporation front. In general, it is necessary to take into account the electron-phonon coupling term to properly describe heat transfer into the material. This has a significant impact on the results for sub-picosecond pulse-widths[3,4], but for large, nanosecond pulse-widths, where there is sufficient time for equilibrium to establish, the two temperatures are commonly assumed to be equal, eliminating the electron-phonon coupling term, and thus, simplifying the system to one equation [7-9].

While direct numerical solutions to one-temperature equation[7,8] as well as the two-temperature coupled equations[6] can be obtained under quite general conditions, the problem is frequently approached analytically by making some simplifying assumptions[1-5,9]. Major advantage in the analytical approach is that it provides better insight into the processes and general features of the results, as long as the simplified model is realistic, and such approximate solutions can be made the starting points for further refinements. Considerable simplifications result from the assumptions that the heat capacity of the thermal electrons and the lattice, and the thermal conductivity remain constant during the process of ablation[1,3,9]. Further assumptions are sometime made to facilitate a solution[1]. Also, the solutions are commonly obtained by separate methods for laser pulse-widths in the femtosecond, picosecond and nanosecond regimes with respective simplifying assumptions[1,2,4,9].

In the present paper, we consider the two-temperature model, which describes the phenomenon of thermal diffusion for all pulse-widths, and approach the problem analytically under the assumptions that the heat capacities of the free electrons and the lattice, and the diffusivity of the electron subsystem remain constant. Although these quantities depend on temperature, particularly the electron heat capacity, these assumptions are commonly used to simplify the calculations[1,3,9]. Approximate solutions so obtained provide adequate insight into the processes and quite frequently, provide adequate description of the experimental behaviour. When the effects of the temperature dependence become significant, the approximate solutions can be made the starting points to include the corresponding corrections. However, we have relaxed some assumptions as follows. Shape of the pulse-width is initially assumed to be Gaussian, which provides an accurate description of the energy distribution in the laser beams used for machining. The results are then generalized for other shapes of the beam for comparison with the results available in the literature. Further, since no pertaining assumptions are made, the solution is valid for lasers with an arbitrary pulse-width, which

includes the physically relevant pulse-widths, ranging from the femtosecond to nanosecond. The present, more general solution possesses the attractive features of the approximate solutions available elsewhere[1], which are recovered under the corresponding assumptions. Average heat penetration depth, the ablation depth and the evolution of the temperatures during ablation are found to be in good agreement with the experimentally observed values, which indicates that the assumptions made here have little effect in the cases considered.

2.0 Thermal diffusion model

In the thermal diffusion model, microscopic processes are ignored and the material is divided into two main subsystems, the thermal electrons and the lattice, which is the remaining bulk. In case of metals, the free electrons absorb the laser energy and are accelerated rapidly acquiring large velocities, with consequent high temperatures. Energetic electrons transfer heat to the lattice subsystem by collisions described by the electron-phonon coupling. This interaction between the two subsystems is represented in the model equations by $g\Delta T$, where ΔT is the temperature difference between the two subsystems and g is the electron-phonon coupling constant[1,5]. Since the bulk, collectively, is more massive than the electrons, it exhibits a slower rise in temperature[1,5]. Based on the relative size of the pulse width, τ_L, and the characteristic electron cooling and lattice heating times, τ_e and τ_i, respectively, the process of metal ablation is commonly divided into three regimes: femtosecond ($\tau_L \ll \tau_e \ll \tau_i$), picosecond ($\tau_e \ll \tau_L \ll \tau_i$) and nanosecond ($\tau_e \approx \tau_i \ll \tau_L$)[4].

Space-time distribution of the electron temperature, T_e, and the average lattice temperature, T_i, can be described, to a good degree of approximation, by the following one-dimensional two-temperature diffusion equations[1,3,4]:

$$\frac{\partial T_e}{\partial t} - \frac{\partial}{\partial \xi} D \frac{\partial T_e}{\partial \xi} = - \frac{T_e - T_i}{\tau_e} + \frac{S}{C_e} \tag{1}$$

$$\frac{\partial T_i}{\partial t} = \frac{T_e - T_i}{\tau_i} \tag{2}$$

together with the boundary conditions

$$T_e(\xi, -\infty) = 0, \quad T_e(\infty, t) = 0, \quad \left.\frac{\partial T_e}{\partial \xi}\right|_{\xi=0} = 0 \tag{3}$$

where the zero of the temperature scale is taken to be at the room temperature, D is the diffusivity of the electron subsystem, $\tau_e = C_e / g$, $\tau_i = C_i / g$, with C_e and C_i being the electron and lattice heat capacities, respectively, and ξ is the coordinate distance in the direction of outward normal to the surface[9]. For a horizontal flat surface, ξ reduces to the vertical coordinate, which will be assumed to be the case for the calculations here. For convenience, the time t is measured in units of the pulse width with the units and the values of other quantities adjusted accordingly. Laser source S, with Gaussian distribution of energy is given by,

$$S(\xi,t) = a_0 \alpha I_0 \exp(-\kappa t^2)\exp(-\alpha\xi) \tag{4}$$

where a_0 is the light absorption coefficient, α is the inverse skin depth, I_0 is the peak laser power and, κ is a laser specific constant. Here we take $\kappa = 4log(2)$ in conformity with the laser used for experimental verification of the present solution. In general, the source term also depends on the coordinates of the plane of the cross section of the laser beam. When this dependence is of significance, it can be included in the present analysis.

The temperatures, defined uniquely by Eqs. (1), (2) and (3), for a large class of source terms including as given by Eq. (4), possess the following additional property:

$$T_e(\xi,+\infty) = 0 \tag{5}$$

in conformity with the physical behaviour of eventual cooling of metal to the room temperature. Proof of the result stated in Eq. (5), although lengthy, follows from standard arguments[10]. In view of this property, it is convenient to obtain the temperatures by first solving the corresponding equations for the Fourier transforms of T_e and T_i defined by,

$$\hat{T}_{e,i}(\xi,\omega) = \frac{1}{\sqrt{2\pi}} \int_{-\infty}^{+\infty} T_{e,i}(\xi,t)\, e^{-i\omega t}\, dt$$

In terms of $\hat{T}_e$ and $\hat{T}_i$, Eqs. (1), (2) and (3) reduce to:

$$\frac{\partial^2 \hat{T}_e}{\partial \xi^2} - \frac{i\omega}{D}\hat{T}_e - \frac{\hat{T}_e - \hat{T}_i}{D\tau_e} = -\frac{a_0 \alpha I(x,y)}{\sqrt{2\kappa} C_e D}\, e^{-\omega^2/4\kappa} e^{-\alpha\xi} \tag{6}$$

$$i\omega\hat{T}_i - \frac{\hat{T}_e - \hat{T}_i}{\tau_i} = 0 \tag{7}$$

and $$\hat{T}_e(\infty,\omega) = 0 \text{ and } \left.\frac{\partial \hat{T}_e}{\partial \xi}\right|_{\xi=0} = 0 \tag{8}$$

respectively. It follows that

$$\hat{T}_i = \frac{1}{1+i\omega\tau_i}\hat{T}_e \tag{9}$$

and

$$\frac{\partial^2 \hat{T}_e}{\partial \xi^2} - \beta^2(\omega)\hat{T}_e = -R\, e^{-\omega^2/4\kappa} e^{-\alpha\xi} \tag{10}$$

with the boundary conditions as stated in Eq. (8). Here

$$\beta^2(\omega) \equiv \frac{1}{D\tau_e}\left[1 - \frac{1}{1+\omega^2\tau_i^2} + i\omega\tau_e\left(1 + \frac{\tau_i/\tau_e}{1+\omega^2\tau_i^2}\right)\right] \tag{11}$$

and

$$R \equiv \frac{a_0 \alpha I(x,y)}{\sqrt{2\kappa} D C_e} = \frac{\alpha F_a}{\sqrt{2\pi} D C_e} \tag{12}$$

where F_a is the laser fluence absorbed by the metal. Eq. (10) is solved by standard methods yielding,

$$\hat{T}_e(\xi,\omega) = \frac{\alpha F_a}{\sqrt{2\pi}DC_e}\frac{1}{\alpha^2-\beta^2(\omega)}\left(-e^{-\alpha\xi}+\frac{\alpha}{\beta(\omega)}e^{-\beta(\omega)\xi}\right)e^{-\omega^2/4\kappa}$$
$$= \frac{F_a}{\sqrt{2\pi}DC_e}\frac{l^2(\omega)}{l^2(\omega)-\gamma^2}\left(-\gamma e^{-\xi/\gamma}+l(\omega)e^{-\xi/l(\omega)}\right)e^{-\omega^2/4\kappa} \quad (13)$$

where $\beta(\omega)$ is the principal branch of $\sqrt{\beta^2(\omega)}$, defined by $\mathrm{Re.}(\beta(\omega))>0$, $l(\omega)=[\beta(\omega)]^{-1}$, and the skin depth $\gamma=\alpha^{-1}$. Eq. (13) together with Eq. (9) determines $\hat{T}_i$:

$$\hat{T}_i(\xi,\omega) = \frac{1}{1+i\omega\tau_i}\left\{\frac{F_a}{\sqrt{2\pi}DC_e}\frac{l^2(\omega)}{l^2(\omega)-\gamma^2}\left(-\gamma e^{-\xi/\gamma}+l(\omega)e^{-\xi/l(\omega)}\right)e^{-\omega^2/4\kappa}\right\} \quad (14)$$

Eqs. (13) and (14) can be generalized to any laser source expressible as $[S'(t)\exp(-\xi/\gamma)]$, yielding the following expressions for the temperatures:

$$T_{e,i}(\xi,t) = \int_{-\infty}^{+\infty} T^{\delta}_{e,i}(\xi,t-\eta)\,S'(\eta)\;d\eta \quad (15)$$

where
$$\hat{T}^{\delta}_i(\xi,\omega) = \frac{\hat{T}^{\delta}_e(\xi,\omega)}{1+i\omega\tau_i} \quad (16)$$

and

$$\hat{T}^{\delta}_e(\xi,\omega) = \frac{1}{\sqrt{2\pi}DC_e}\left(\frac{l^2(\omega)}{l^2(\omega)-\gamma^2}\right)\left(-\gamma e^{-\xi/\gamma}+l(\omega)e^{-\xi/l(\omega)}\right) \quad (17)$$

Relative behaviour of the electron and lattice temperatures in different pulse-width regimes, which is usually inferred from the solution of Eq. (2), can be deduced from Eq. (9), or from the solutions stated in Eqs. (13) to (17). For pulse-widths in the nanosecond range, $\tau_i \ll 1$ in units of pulse-width, and thus $|\omega\tau_i| \ll 1$, i.e., $(1+i\omega\tau_i)\approx 1$, except for large values of $|\omega|$, where the values of $\hat{T}_{e,i}(\xi,\omega)$ are quite small, with small contribution to the integral defining the inverse Fourier transform. Therefore, for the large pulse-widths, the electron and the lattice temperatures may be taken to be equal, to a good degree of accuracy. This approximation is commonly used to reduce the two-temperature coupled equations to a single equation, with consequent simplifications[4,7-9]. Qualitative features of the temperatures for the sub-picosecond pulse-widths used in the literature[1-5] can also be deduced from the present results by similar straightforward arguments. However, for the shorter pulse-widths, the electron-phonon interaction term becomes significant[3], making it necessary to solve the two-temperature equations or their simplified forms[4]. The present solutions are valid, and about equally convenient, for all pulse-widths.

3.0 Results and discussion

In this section, we calculate the heat penetration depth, the temperatures and the ablation depth using the results of Sec. 2. The temperatures are obtained directly by taking the inverse Fourier transforms of $\hat{T}_e(\xi,\omega)$ and $\hat{T}_i(\xi,\omega)$. An Arrhenius type equation deduced in terms of the vapour pressure, determines the ablation depth from the knowledge of the lattice temperature $\hat{T}_i(\xi,\omega)$ [1,5]. The heat penetration depth is identified from an approximate expression for $T_i^{\delta}(\xi,t)$.

3.1 Heat penetration depth

We show below that if $l(\omega)$ is replaced with a constant $\bar{l}$ in the inverse Fourier transform representation of $T_i^{\delta}(\xi,t)$, then the approximate expressions of the temperatures in Ref. [1] are recovered, with the corresponding source term. In addition to illustrating the features of the present solutions, this also provides an insight into the approximations used in the literature and motivates a physical interpretatio of $l(\omega)$. The approximation under consideration to $T_i^{\delta}(\xi,t)$ is given by

$$\begin{aligned} T_i^{\delta}(\xi,t) &= \frac{1}{\sqrt{2\pi}}\int_{-\infty}^{\infty} d\omega\, e^{i\omega t}\, \frac{\hat{T}_e^{\delta}(\xi,l(\omega))}{1+i\omega\tau_i} \\ &\simeq \frac{1}{\sqrt{2\pi}}\int_{-\infty}^{\infty} d\omega\, e^{i\omega t}\, \frac{\hat{T}_e^{\delta}(\xi,\bar{l})}{1+i\omega\tau_i} \\ &= \frac{1}{DC_e}\frac{\bar{l}^2}{\bar{l}^2-\gamma^2}\left\{-\gamma e^{-\xi/\gamma}+\bar{l}e^{-\xi/\bar{l}}\right\}\frac{\exp(-t/\tau_i)h(t)}{\tau_i} \end{aligned} \tag{18}$$

where $h(t)$ is the Heaviside step function. For clarity of comparisons, the pulse-width τ_L will be explicitly shown in the following.

The source term in Ref. [1] was taken to be

$$S(\xi,t) = A\alpha\, \exp(t/\tau_L)\, h(-t) \tag{19}$$

Since the source term given by Eq. (19) falls to zero discontinuously at time equal to zero, it is unrealistic. We have considered it here to illustrate the properties of the present treatment, which is valid for considerably more general source terms.

From Eqs. (18), (19) and (15), it follows that

$$T_i(\xi,t<0) = \frac{F_a}{C_e D}\frac{\bar{l}^2}{\bar{l}^2-\gamma^2}\left(-\gamma e^{-\xi/\gamma}+\bar{l}e^{-\xi/\bar{l}}\right)\frac{1}{\tau_L+\tau_i}e^{t/\tau_L}$$

$$T_i(\xi,t>0) = \frac{F_a}{C_e D}\frac{\bar{l}^2}{\bar{l}^2-\gamma^2}\left(-\gamma e^{-\xi/\gamma}+\bar{l}e^{-\xi/\bar{l}}\right)\frac{1}{\tau_L+\tau_i}e^{-t/\tau_i}$$

where the absorbed fluence is given by[1] $F_a = A\alpha\tau_L$. The equation for the temperature for time below zero agrees with that in Ref. [1] with $\bar{l}$ termed the heat penetration depth. For the positive times, for t and τ_L in the femtosecond regime, $\exp(-t/\tau_i)\approx 1$, and

$\frac{\tau_i}{\tau_L + \tau_i} \approx 1$. By setting $\bar{l} \approx \sqrt{D\tau_e}$, which is approximately the heat penetration depth defined in Ref. [1], and using the fact that $\tau_e / C_e = g = \tau_i / C_i$, the same approximation for the equilibrium temperature of the lattice subsystem is obtained as given by Eq. (24) of Ref. [1], which is,

$$T_i(\xi, t > 0) \simeq \frac{F_a}{C_i} \frac{1}{\bar{l}^2 - \gamma^2} \left(-\delta e^{-\xi/\gamma} + \bar{l} e^{-\xi/\bar{l}} \right)$$

These considerations show that the approximation used in deducing Eq. (18) is consistent with the approximations of Ref. [1], which is to replace $l(\omega)$ by a constant $\bar{l}$ in the integrand in the inverse Fourier transform of $T_i^{\delta}(\xi, t)$. In view of this, $l(\omega)$ may be considered the spectral distribution of the heat penetration depth, and $\bar{l}$, the mean value of the distribution $l(\omega)$. With this identification, we have

$$\bar{l} \simeq \lim_{\sigma \to \infty} \frac{1}{2\sigma} \int_{-\sigma}^{+\sigma} l(\omega)\, d\omega \tag{20}$$

Since $\left| \hat{T}_i(\xi, \omega) \right| \leq \exp(-\omega^2 / 4\kappa)$, $\bar{l}$ is quite accurately determined by Eq. (20) with a reasonably large fixed value of σ, without taking the limit. We have found it sufficient to set $\sigma = 4\kappa$, yielding

$$\bar{l} = \frac{1}{8\kappa} \int_{-4\kappa}^{+4\kappa} l(\omega)\, d\omega \tag{21}$$

It was verified numerically that a larger interval makes no noticeable difference in the results. Since Im. $\beta(\omega)$ is an odd function of ω Im.$[l(\omega)]$ is also odd in $l(\omega)$ and therefore the imaginary component will vanish in the integral over a symmetrical interval, and hence, $\bar{l}$ is real, as the value of the heat penetration depth should be.

It is known both experimentally and theoretically that the heat penetration depth in the sub-nanosecond regime is approximately constant, equal to $\sqrt{D\tau_e}$, while it behaves in proportion to $\sqrt{\tau_L}$ in the nanosecond regime[1-3]. Figure 1 compares the behaviour of $\bar{l}$ obtained from Eq. (21) with the values reported in Ref. [1] with respect to the pulse-width. Diffusivity, D for both curves was estimated by using the formula $D \approx v_F^2 \tau_R / 3$ where τ_R is the electron relaxation time and v_F is the Fermi velocity [1]. We assumed that τ_R is minimum, which is approximately, a / v_F where a is an average inter-atomic distance ($a \approx 4$ Å for Cu) and v_F is the Fermi velocity. This is adequate within the framework of the present approximations. The characteristic lattice heating time and the electron-phonon coupling constant, g are about 34 ps and 10^{17}Wm^{-2}K^{-1} respectively[1,3]. The electron heat capacity is given by $C_i \tau_e / \tau_i \approx 10^{-5} C_i$. Apart from an offset, the behaviour of $\bar{l}$ as given by Eq. (21) is about the same as the heat penetration depth predicted by Eqs. (13), (14) and (20) of Ref. [1] below 100 ps. For all pulse-widths,

the present values are less than the values reported in Ref. [1], for nanosecond regime more so than the lower pulse-widths. Both of these approximations indicate that the heat penetration depth has a very weak dependence on the pulse-width in the sub-nanosecond regime and a strong dependence in the nanosecond regime. In the nanosecond regime, both sets of values increase approximately in proportion to $\sqrt{\tau_L}$, with constant of proportionality depending on other parameters, in agreement with other observations[2-6].

3.2 Time evolution of temperatures

The electron temperature was obtained by evaluating the inverse Fourier transform of $\hat{T}_e(\xi,\omega)$, and the lattice temperature $T_i(\xi,t)$ was evaluated by convoluting $T_e(\xi,t)$ with $[h(t)\exp(-t/\tau_i)/\tau_i]$, in conformity with Eq. (9). The inverse Fourier transform was obtained using the FFT routine in Matlab and the electron heat capacity was taken to be equal to $(3N_e k_B/2)$, ensuring the electron cooling time of the order of picoseconds.

Figures 2, and 3 show the lattice and electron temperatures in nanosecond and femtosecond regimes, respectively. As expected, the electron and lattice temperatures are almost equal for all times in the laser pulse-width in the nanosecond range. The temperature values for 100 fs pulse- width agree qualitatively with those reported in Refs. [2] and [6]. In this case, the lattice temperature is considerably less than the electron temperature at lower times but they both converge to each other as the time increases, indicating the approach of a thermal equilibrium. After the thermal equilibrium has been established, the temperatures, which are about equal, decrease at a very slow rate, validating the common assumption of a constant lattice temperature at intermediate times during the ablation phase by the femtosecond lasers.

3.3 Ablation depth

The ablation depth can be estimated by integrating the velocity of the evaporation front during ablation, given by[1]

$$v = v_0 \exp(-H_{vap}/C_i T_i) \qquad (22)$$

where H_{vap} is the heat of vaporization per unit volume and v_o is of the order of sound velocity in the metal in its condensed state[1,5]. The duration of ablation is known to be of the order of electron-ion thermalization time as stated in Ref. [1], and thus, it is sufficient to integrate the velocity on the interval $[-\infty,\tau_i]$. The laser fluence was varied from 1mJ/cm^2 to 10 J/cm^2 and pulse-width was taken to be equal to 150 fs.

The calculated ablation depth is plotted in Figure 4 as a function of the fluence on a logarithmic scale. As indicated by the dotted lines, the curve is approximated well by two straight lines, up to the fluence of about 2 J/cm^2, demonstrating two different logarithmic variations in the two fluence regions. At higher values of the fluence, the behaviour deviates from logarithmic. These qualitative deductions are in agreement with the conclusions based on the experimental observations[1].

The case where $C_e \approx N_e k_B/3$, the electron cooling time is about 10^5 times its minimum value, and the ablated depth is practically zero for the same range of fluence

values as above. This is expected since there is a long time delay for the electron energy to be transferred to the lattice subsystem, which eventually causes ablation. Furthermore the higher value of C_e significantly reduces the electron temperature that can be achieved for a given fluence; in this case it reduces the temperature by a factor of approximately 10^5. Thus, the amount of fluence needed for ablation increases with an increase in the electron heat capacity. For pulse-widths in the nanosecond range, the electron and lattice subsystems are in an approximate state of equilibrium, and the electron heat capacity is of the same order as the relatively large lattice heat capacity. Therefore, larger fluence values are required for ablation with the nanosecond pulse-width lasers, as also observed elsewhere [1-6].

4.0 Concluding remarks

An analytical solution of the two-temperature model describing ablation of metals with Gaussian laser source is obtained under the assumptions that the lattice heat capacities and the thermal conductivity of the electron and lattice subsystems remain approximately constant during the process. An expression for the lattice temperature due to the delta function excitation was also obtained, which may be convoluted with a general laser source to obtain the resulting lattice temperature. The solution was shown to reduce to a previously reported approximate solution under the corresponding assumptions[1]. Sample calculations show a good agreement with several observations of the heat penetration depth, ablation depth and the temperature behaviour reported elsewhere[1-4,6], and confirms several intuitive assumptions made in the literature.

For a more complete description of the process, it is necessary to include the effects of a moving boundary, non-constant heat capacities and thermal conductivities as well as the diffusivity together with the further refinements of the subsystems. While these effects may become significant in some situations, for a large class of cases, the results obtained by the direct numerical methods that include these effects[6] are in close agreement with the present results. In cases when it may become necessary to improve upon the approximations of this article, the solution obtained here still provides an adequate insight into the process and the qualitative behaviour of the results. Also, the present solution may be made a starting point for more accurate calculations.

Acknowledgements

The authors are thankful to Mr. M. Islam, Director, Production Technology Research, IMTI, and to Dr. S. K. Nikumb, Group Leader, Precision Fabrication Processes, IMTI, for their continued support in this work.

References

1. Nolte, S., Momma, C., Jacobs, H., Tunnermann, A., Chichkov, B.N., Wellegehausen, B. and Welling, H. Ablation of metals by ultrashort laser pulses. J. Opt. Soc. Am. B. 14: 1997; pp. 2716-2722.

2. Wellershoff, S.-S., Hohlfeld, J., Gudde, J., Matthias E. The role of electron-phonon

coupling in femtosecond laser damage of metals. Applied Physics A. 69: 1999; pp. S99-S107

3. Corkum, P.B., Brunel, F. and Sherman, N.K. Thermal response of metals to ultrashort-pulse laser excitation. Phys. Rev. Lett. 61: 1988; pp. 2886-2889.

4. Chichkov, B.N., Momma, C., Nolte, S., von Alvensleben, F. and Tunnermann, A. Femtosecond, picosecond and nanosecond laser ablation of solids. Appl. Phys. A. 63: 1996; pp. 109-115.

5. Baüerle, D., *Laser Processing and Chemistry*, 3rd edition, Springer, New York, 2000.

6. Chen, J.K., Beraun, J.E., Numerical Study of Ultrashort Laser Pulse Interactions with Metal Films. Numerical Heat Transfer, Part A, 40: 2001; pp. 1-20.

7. R.F. Wood and G.E. Jellison, Jr., Melting model of pulsed laser processing, in Semiconductors and semimetals, Vol. 23 (Academic Press, New York, 1984) pp.166-250.

8. Wood, R.F. and Giles, G.E. Macroscopic theory of pulsed-laser annealing. I. Thermal transport and melting. Phys. Rev. B. 23: 1981; pp. 2923-2942.

9. S.R. Vatsya, E.V. Bordatchev and S.K. Nikumb, Geometrical modeling of surface profile formation during laser ablation of materials, Submitted for publication.

10. S.R. Vatsya, Asymptotic limit of the solutions of the two-temperature thermal diffusion model of laser-metal interactions, Internal Report, IMTI-TR-013 (2002/09).

List of Figures

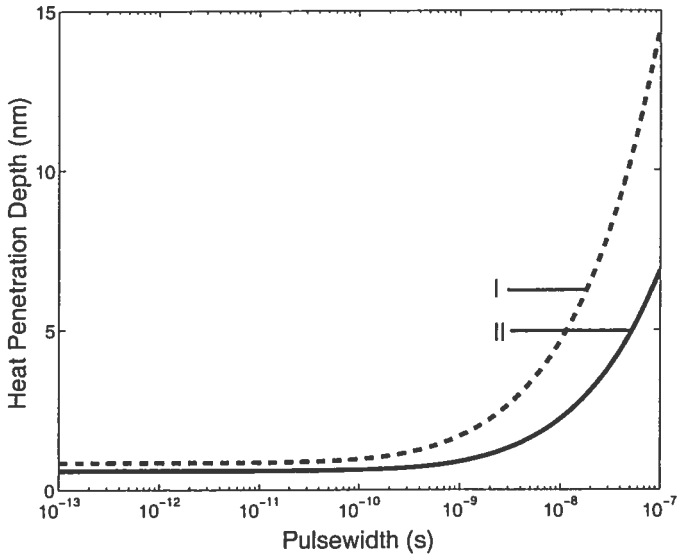

Figure 1.

S.R. Vatsya and Kuljit S. Virk

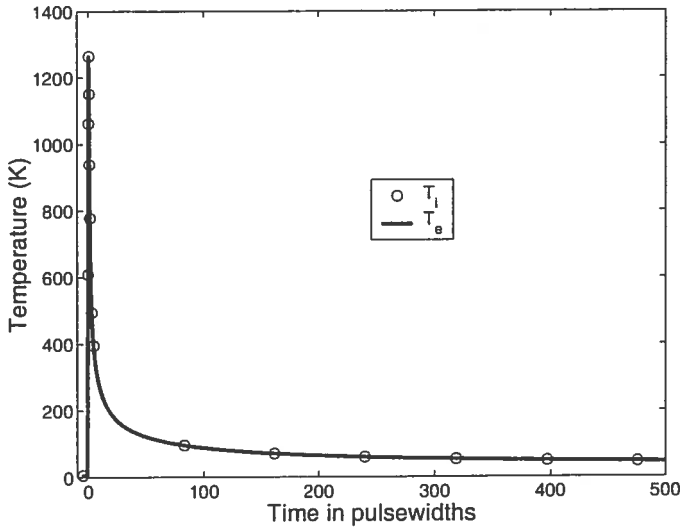

Figure 2.

S.R. Vatsya and Kuljit S. Virk

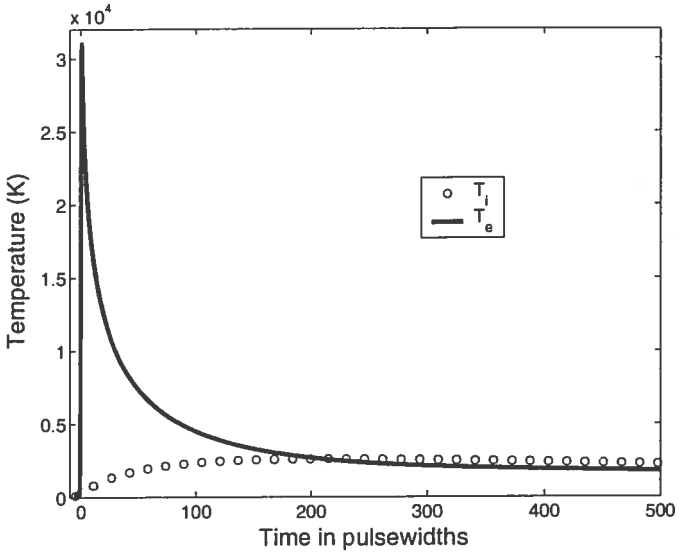

Figure 3.

S.R. Vatsya and Kuljit S. Virk

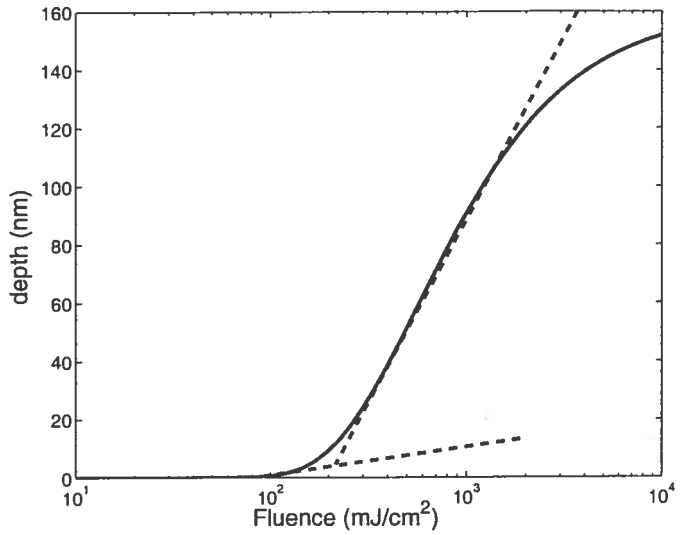

Figure 4

S.R. Vatsya and Kuljit S. Virk